

## Simulated Local and Remote Biophysical Effects of Afforestation over the Southeast United States in Boreal Summer\*

GUANG-SHAN CHEN, MICHAEL NOTARO, AND ZHENGYU LIU

*Center for Climatic Research, University of Wisconsin—Madison, Madison, Wisconsin*

YONGQIANG LIU

*Center for Forest Disturbance Science, USDA Forest Service, Athens, Georgia*

(Manuscript received 14 June 2011, in final form 31 October 2011)

### ABSTRACT

Afforestation has been proposed as a climate change mitigation strategy by sequestering atmospheric carbon dioxide. With the goal of increasing carbon sequestration, a Congressional project has been planned to afforest about 18 million acres by 2020 in the Southeast United States (SEUS), the Great Lake states, and the Corn Belt states. However, biophysical feedbacks of afforestation have the potential to counter the beneficial climatic consequences of carbon sequestration. To assess the potential biophysical effects of afforestation over the SEUS, the authors designed a set of initial value ensemble experiments and long-term quasi-equilibrium experiments in a fully coupled Community Climate System Model, version 3.5 (CCSM3.5). Model results show that afforestation over the SEUS not only has a local cooling effect in boreal summer [June–August (JJA)] at short and long time scales but also induces remote warming over adjacent regions of the SEUS at long time scales. Precipitation, in response to afforestation, increases over the SEUS (local effect) and decreases over adjacent regions (remote effect) in JJA. The local surface cooling and increase in precipitation over SEUS in JJA are hydrologically driven by the changes in evapotranspiration and latent heat flux. The remote surface warming and decrease in precipitation over adjacent regions are adiabatically induced by anomalous subsidence. Our results suggest that the planned afforestation efforts should be developed carefully by taking account of short-term (local) and long-term (remote) biophysical effects of afforestation.

### 1. Introduction

Forest ecosystems have great economic, social, and aesthetic value for humans by providing food, medicinal, and forest products and improving water quality and soil resources (Bonan 2008). In addition, forest ecosystems sequester billions of tons of carbon globally every year (Canadell and Raupach 2008). Therefore forestry, such as afforestation, reforestation, and forest management, has been proposed as a potential climate change mitigation strategy (Anderson et al. 2010), although it is hard to determine how much of the forestry can

mitigate atmospheric CO<sub>2</sub> warming (Canadell and Raupach 2008; Pacala and Socolow 2004). A Congressional project has been planned to afforest about 18 million acres by 2020 in the Southeast United States (SEUS), the Great Lake states, and the Corn Belt states (Watson 2009). The SEUS consists of 13 states from Texas to the Atlantic coast and from Florida to Virginia, with 40% of the nation's forests within just 24% of the United States land area (American Forest Congress 1996). The primary aim of this project is to mitigate the ongoing global warming due to the greenhouse effect, projected by many global general circulation models (GCMs) (Solomon et al. 2007). However, afforestation also affects the climate through multiple biophysical feedbacks, such as by modifying Bowen ratio, surface roughness length, and surface albedo (Foley et al. 2003; Field et al. 2007; Bonan 2008; Chapin et al. 2008; Anderson et al. 2010). These biophysical feedbacks, in some cases, may reduce or eliminate the beneficial effects of carbon sequestration (Anderson et al. 2010).

---

\* Nelson Institute Center for Climatic Research Publication Number 1075.

---

*Corresponding author address:* Guang-Shan Chen, Center for Climatic Research, University of Wisconsin—Madison, 1225 West Dayton St., Madison, WI 53705.  
E-mail: gchen9@gmail.com

Currently, it is difficult to evaluate these biophysical feedbacks of vegetation on climate through observations, even though some studies have applied satellite-based indices to assess present-day vegetation feedbacks on global or regional climate (Kaufmann et al. 2003; Liu et al. 2006; Notaro and Liu 2006, 2008). Most of our understandings on how vegetation affects climate come from model simulations. Three mechanisms [albedo, evapotranspiration (ET), and roughness] have been proposed to explain the biophysical effects of vegetation on climate (Oyama and Nobre 2004). Vegetation generally has a lower albedo compared to bare or snow-covered grounds, resulting in an increase in energy absorbed by the surface, an increase in surface air temperature, and possibly an increase in precipitation (albedo mechanism) (Charney 1975). Vegetation is efficient in evapotranspiration and partitioning more energy into latent heat, resulting in a decrease in surface temperature and possibly an increase in precipitation (evapotranspiration mechanism) (Shukla and Mintz 1982). High roughness length of vegetation, on one hand, results in an increase in turbulent fluxes (latent heat and sensible heat), thus reducing surface air temperature. On the other hand, it results in more mass convergence associated with anomalous lower pressure, increasing upward moisture transport and convective cloud, thus increasing precipitation and lowering surface temperature (roughness mechanism) (Sud et al. 1988).

The sign of each of these mechanisms and which one dominates varies by geographical regions, seasons, and climate variables interested. Generally, climate model simulations show that the albedo mechanism dominates on temperature change at high latitudes with trees masking of snow for boreal forests (Betts 2000; Govindasamy et al. 2001; Notaro and Liu 2008); and the evapotranspiration mechanism dominates on temperature at low latitudes with high rates of evapotranspiration for tropical forests (Eltahir and Bras 1993; Lean and Rowntree 1993; Costa and Foley 2000; Osborne et al. 2004; Gibbard et al. 2005). However, potential biophysical feedbacks of temperate forests in many midlatitude regions are highly uncertain, including the SEUS (Bonan 2008; Anderson et al. 2010).

Statistical analysis of observed vegetation feedbacks in the United States hints that afforestation leads to a cooling on surface temperature and an increase in precipitation (Notaro and Liu 2006). But modeling results do not agree on the afforestation effects on temperature and precipitation over the SEUS. Xue et al. (1996) found a summer cooling of up to 2°C because of an increased latent heat flux and an increase in precipitation in the eastern United States by replacing the

crop vegetation with broadleaf deciduous trees across the country in a GCM model. Using a regional climate model, Copeland et al. (1996) showed that forest cooled the eastern United States by 0.22 K and decreased precipitation by 0.12 mm day<sup>-1</sup> in July, compared to crop vegetation. Baidya Roy et al. (2003) and Jackson et al. (2005) also found afforestation typically decreased summer surface air temperature over the SEUS, using mesoscale models. But other studies suggested that the temperate forests in the eastern United States increased summer temperature (e.g., Bonan 1997; Oleson et al. 2004).

Besides the aforementioned uncertainties in biophysical feedbacks of temperate forest, an increasing number of studies indicated the potential remote effects of vegetation changes by teleconnections in GCMs (Chase et al. 2000; Werth and Avissar 2002; Avissar and Werth 2005; Hasler et al. 2009; Snyder 2010). Very recently, Liu (2011) evaluated the potential role of the Congressional afforestation project over the SEUS using a regional climate model by replacing agriculture lands with trees. It was found that precipitation increased in the eastern portion of the SEUS and decreased in the western portion of the SEUS in summer. Surface air temperature decreased in the SEUS in summer, but only slightly. However, in this simulation, only the short-term afforestation effects were studied and the dynamical ocean effects and possible teleconnections were eliminated with the RegCM.

To have a better evaluation on the planned afforestation over the SEUS, the following questions need to be addressed in a state-of-the-art fully coupled GCM with a dynamic vegetation and a finite volume dynamical core. 1) What are the potential short-term and long-term local biophysical effects of afforestation over the SEUS? 2) What are the potential remote biophysical effects of afforestation over the SEUS? In this paper, these questions are answered with 80 initial value ensemble experiments and two long quasi-equilibrium experiments by using a fully coupled earth system model with dynamic vegetation. The model used and experiments are described in section 2. Results are presented in section 3. The summaries and discussion are presented in section 4.

## 2. Model description and experiments design

### *a. Model description*

The model used in this paper is the National Center for Atmospheric Research (NCAR) Community Climate System Model, version 3.5 (CCSM3.5) (Gent et al. 2010). CCSM3.5 is an interim version between CCSM3 and

CCSM4 or NCAR Community Earth System Model version 1.0 (CESM1). The fully coupled model has five components, including the Community Atmosphere Model (CAM) with 26 vertical layers, Community Land Model (CLM) with dynamic vegetation, Parallel Ocean Program (POP) with 60 vertical layers, Community Sea Ice Model (CICE), and Community Land Ice Sheet Model (CLSM). There are 10 soil layers and 10 plant functional types (PFTs) generated in the dynamic vegetation model, including seven types of trees and three types of grasses with annual processes based on the Lund–Potsdam–Jena (LPJ) Dynamic Global Vegetation Model (DGVM) (Levis et al. 2004). In this study, the finite-volume dynamical core (Lin 2004) (not a spectral dynamical core) is chosen and the horizontal resolution used is  $1.9^\circ$  (latitude)  $\times$   $2.5^\circ$  (longitude) for CAM and CLM.

CCSM3.5 has numerous improvements comparing with its predecessors (Oleson et al. 2008; Stöckli et al. 2008; Gent et al. 2010). In CAM, convective scheme includes both shallow convection (Hack 1994) and deep convection (Zhang and McFarlane 1995). In CLM, the partitioning of evapotranspiration (ET) between canopy evaporation, transpiration, and soil evaporation is significantly improved, resulting in wetter soils, reduced water stress on plants, increased transpiration, enhanced photosynthesis, and a better representation of the annual cycle of total water storage (Oleson et al. 2008). A resistance term is added to reduce excessive soil evaporation, while scaling of the canopy interception is included (Lawrence et al. 2007) to alleviate the excessive interception (Hack et al. 2006).

### b. Experiments

A 100-yr modern-day control simulation of CCSM3.5 is generated from a quasi-equilibrium state (Notaro and Gutzler 2011; Notaro et al. 2011a,b). In the control run, the vegetation used is the model-generated quasi-equilibrium potential natural vegetation. The tree cover limitation is 95% for each grid. A sensitivity experiment is designed with the same vegetation as in the control run, except that the tree cover limitation is capped to 65% in the SEUS region. We note that 65% tree cover is chosen from the current tree cover over the SEUS (Hansen et al. 2000). The sensitivity experiment runs for 80 yr, starting from year 20 of the control run. Given the length of the two simulations, the simulations reach quasi equilibrium. The last 50-yr data of the control run and the sensitivity experiment are analyzed in this study. We refer to the control simulation as the high tree cover experiment (HTC) and the sensitivity experiment as the low tree cover experiment (LTC). A comparison of the HTC with the LTC yields the equilibrium responses to afforestation.

To assess the initial climatic responses to afforestation over the SEUS, a set of 80 initial value ensemble experiments (ENS) is also performed with the same vegetation as in the LTC. For each member of the ensembles, the model starts with a restart file from the HTC experiment over the last 80 yr, respectively, with 2 yr in duration. We note that the model updates the tree cover at the end of the first year of each experiment. So the last year data of each ensemble experiment is analyzed. This ensemble approach is used in vegetation model simulations to get rid of initial condition uncertainty and to increase signal to noise ratio by ensemble average (Baidya Roy et al. 2003; Notaro and Liu 2008; Notaro and Gutzler 2011; Notaro et al. 2011a,b). The initial value ensemble approach shows the climate responses at the short-term time scale that may be different with the long-term quasi-equilibrium responses because of the slow processes in the climate system.

For the purpose of this study, the results are presented and described from the perspective of afforestation effects rather than deforestation effects (HTC-LTC, or HTC-ENS). Student's *t* tests are used to identify the statistical significance of the differences between the simulations. All differences in the text are statistically significant at the  $p < 0.1$  significant level, unless identified otherwise.

### c. Observation and reanalysis

Simulated temperature and precipitation are compared with the UDeI\_AirT\_Precip data ([http://www.esrl.noaa.gov/psd/data/gridded/data.UDeI\\_AirT\\_Precip.html](http://www.esrl.noaa.gov/psd/data/gridded/data.UDeI_AirT_Precip.html)). Simulated vegetation types are compared against the potential natural vegetation dataset of Ramankutty and Foley (1998).

## 3. Results

### a. Mean simulated temperature, precipitation, and vegetation

CCSM3.5 generally simulates a reasonable climatology for global monsoon systems, although there are wet biases for precipitation (Notaro et al. 2011a). Figure 1 also shows that the model simulates reasonable seasonal cycles of temperature and precipitation in the SEUS (the study region shown in Fig. 2). The simulated and observed seasonal cycle of temperature agree quite well with a peak in July, though the simulated temperature in summer (winter) is about  $1^\circ\text{C}$  ( $2^\circ\text{C}$ ) higher than the observation (Fig. 1a). The seasonal timing of precipitation is also well simulated. However the simulated precipitation is about 18% higher in summer and

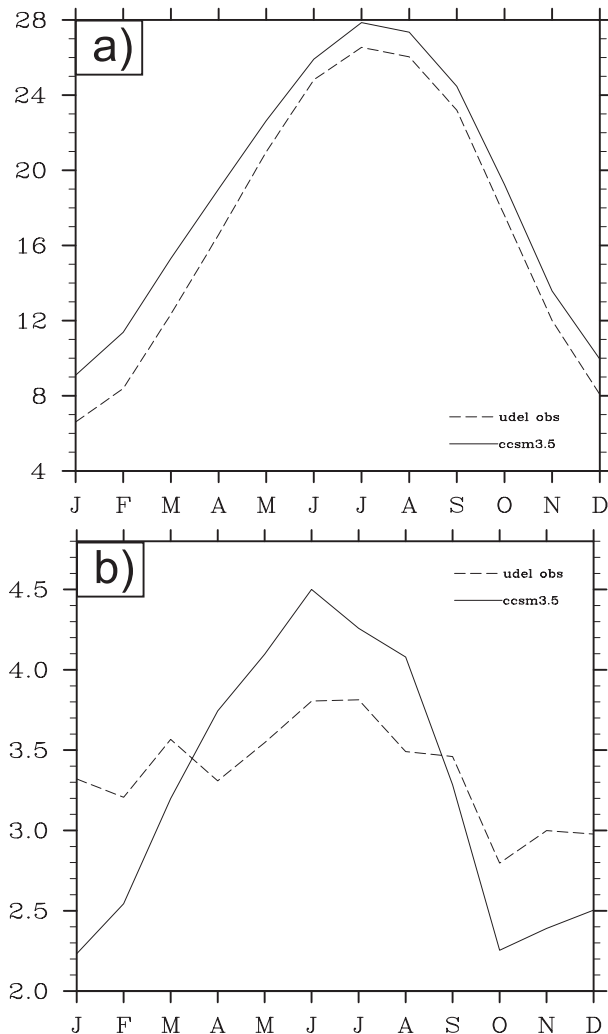


FIG. 1. Climatological seasonal cycle of (a) temperature ( $^{\circ}\text{C}$ ) and (b) precipitation ( $\text{mm day}^{-1}$ ) averaged over the SEUS. Solid lines show the simulated results in the HTC experiment. Dashed lines show the observed data. The SEUS region is shown in Fig. 2.

about 30% lower in winter (Fig. 1b). The model exaggerates the seasonal cycle of precipitation. We note that the reasons for the discrepancies between the model and the observation are out of the scope of the paper.

The simulated vegetation types generally agree with the potential natural vegetation dataset of Ramankutty and Foley (1998) in the SEUS, except the north part of SEUS (north of  $35^{\circ}\text{N}$ ). The model simulates temperate evergreen/deciduous mixed trees over the north part of SEUS (north of  $35^{\circ}\text{N}$ ), while the dataset (Ramankutty and Foley 1998) suggests the primary vegetation type is temperate deciduous tree. The model exaggerates the distribution of temperate evergreen trees over the north part of the SEUS because of the wet bias in precipitation and the warming bias in temperature. However, we mainly focus on afforestation effect in summer, which

makes the exaggeration of temperature evergreen trees over the north part of SEUS less of a concern.

### b. Vegetation change

The area-averaged total tree cover is higher by 24% over the SEUS in HTC experiment than LTC (Table 1, Fig. 2a). Because of the competition between the biomes, the grass cover is decreased by 25% in HTC (Table 1, Fig. 2b). Total vegetation cover is not changed (Table 1). The total tree cover change is associated with the change in temperate needleleaf evergreen trees (+13%), temperate broadleaf deciduous trees (+7%), and temperate broadleaf evergreen trees (+5%) (Table 1). CCSM3.5 only simulates natural vegetation types and not crops, so we approximate afforestation over the SEUS by tree versus grass. We note that the magnitude change of vegetation is underestimated because of the lack of crop land, where the model plants trees. With afforestation over the SEUS, the total leaf area index (LAI) increases in June–August (JJA) (annually) by  $+1.60 \text{ m}^2 \text{ m}^{-2}$  ( $+1.42 \text{ m}^2 \text{ m}^{-2}$ ) (Table 2). Correspondingly, the surface albedo decreases in JJA (annually) by  $-0.019$  ( $-0.022$ ) (Table 2). The top canopy height also increases annually by  $+8.73 \text{ m}$  with grasses replaced by trees (Table 2). The top canopy is about two times higher in HTC (15 m) than that in LTC (6 m). In response to the increase in the canopy height, surface stress statistically increases throughout the year by  $+0.007 \text{ kg m}^{-1} \text{ s}^{-2}$  (Table 2).

### c. Effects of afforestation

On the annual average, afforestation has no statistically significant effects on surface air temperature and precipitation over the SEUS, even though it significantly affects the hydrological cycle by increasing total evapotranspiration ( $+0.06 \text{ mm day}^{-1}$ ) (Table 2). This is mainly attributed to an annual increase in vegetation transpiration, which results in a decrease in total soil moisture ( $-0.007 \text{ mm}^3 \text{ mm}^{-3}$ ) (Table 2). However, afforestation leads to a significant reduction in surface air temperature ( $-0.30^{\circ}\text{C}$ ) and a significant increase in precipitation ( $+0.23 \text{ mm day}^{-1}$ ) over the SEUS during summer (Table 2). Table 2 also shows that the largest responses of temperature, precipitation, and evaporation/latent heat happen in JJA. Therefore, in the subsequent text, we only focus on afforestation effects on climate in JJA and explore the corresponding mechanism of vegetation feedbacks.

#### 1) EFFECT OF AFFORESTATION ON HYDROLOGICAL CYCLE

In summer, precipitation increases in both the short term and the long term over the SEUS (Figs. 3a,b). In the

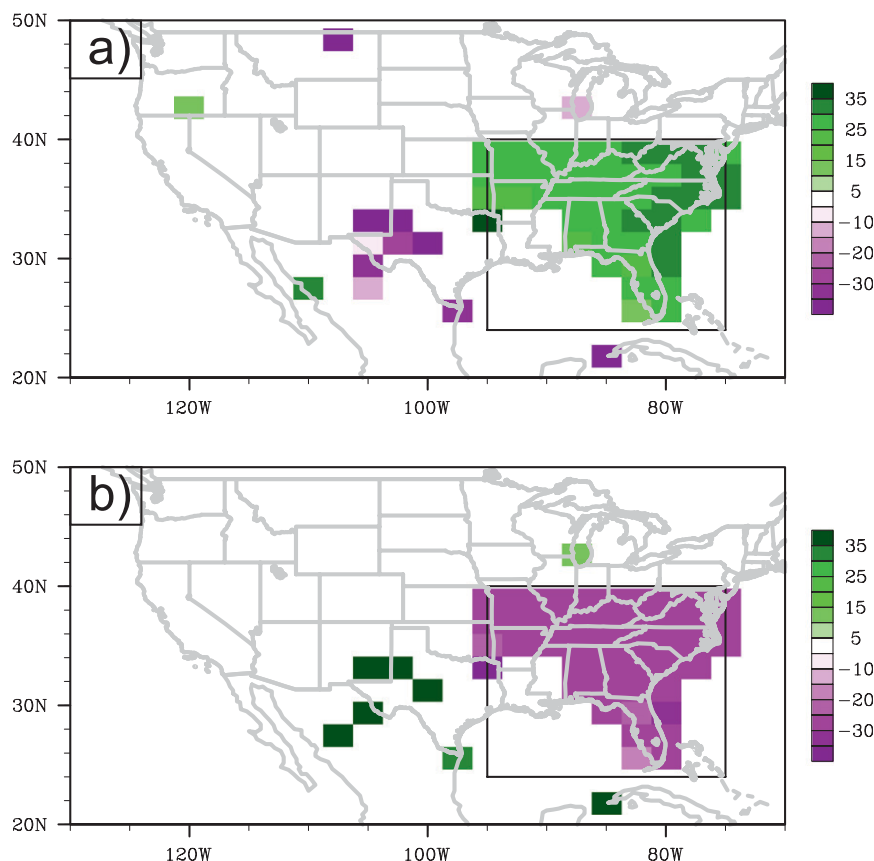


FIG. 2. Difference (HTC – LTC) in percentage cover of (a) total tree and (b) total grass. The box indicates the SEUS region.

long term, precipitation increases by  $+0.23 \text{ mm day}^{-1}$  over the SEUS, which is mainly attributed to convective precipitation ( $+0.21 \text{ mm day}^{-1}$ ) (Table 2). In the short term, precipitation increases almost the same as in the long term. The change in precipitation could be mainly explained by the roughness mechanism. The surface roughness increases, as a function of canopy height. Through the roughness mechanism, low-level mass convergence increases. At low levels, there is an anomalous cyclonic circulation over the SEUS (Figs. 3a,b). At 500 hPa, vertical velocity also indicates anomalous ascent ( $-0.002 \text{ Pa s}^{-1}$ ) over the SEUS (Table 2,

Fig. 4a). With this enhanced ascent, more convective cloud is formed ( $+0.003$ ) (Table 2, Fig. 4b) and total cloud cover increases by  $+0.017$  (Table 2, Fig. 4c). Precipitable water increases by  $+0.70 \text{ kg m}^{-2}$  (Table 2). Therefore, both convective precipitation and total precipitation increase. The evapotranspiration mechanism also can help explain the increase in precipitation. With afforestation and the associated increase in LAI, canopy transpiration and evaporation increase by  $+0.25 \text{ mm day}^{-1}$  and  $+0.15 \text{ mm day}^{-1}$ , while ground evaporation decreases by  $-0.28 \text{ mm day}^{-1}$  (Table 2). As a result, total evapotranspiration increases by  $+0.11 \text{ mm day}^{-1}$ .

TABLE 1. Percentage cover of vegetation types in HTC, LTC, and ENS.

|                                | HTC | LTC | ENS | Long-term (HTC – LTC) | Short-term (HTC – ENS) |
|--------------------------------|-----|-----|-----|-----------------------|------------------------|
| Total vegetation               | 99  | 100 | 96  | –1                    | 3                      |
| Total trees                    | 85  | 61  | 60  | 24                    | 25                     |
| Total grasses                  | 14  | 39  | 36  | –25                   | –22                    |
| Temperate needleleaf evergreen | 34  | 21  | 25  | 13                    | 9                      |
| Temperate broadleaf evergreen  | 25  | 20  | 18  | 5                     | 7                      |
| Temperate broadleaf deciduous  | 26  | 19  | 17  | 7                     | 9                      |
| C3 grass                       | 14  | 39  | 36  | –25                   | –22                    |



TABLE 2. Annual and seasonal differences (HTC – LTC) for the selected 32 variables, averaged across the SEUS, with bold font indicating statistically significant differences at  $P < 0.1$ . January–December (ANN), March–May (MAM), JJA, September–November (SON), and December–February (DJF) are shown.

| Variable                             | Units                            | ANN           | DJF           | MAM           | JJA           | SON           |
|--------------------------------------|----------------------------------|---------------|---------------|---------------|---------------|---------------|
| Total leaf area index                | $\text{m}^2 \text{m}^{-2}$       | <b>1.42</b>   | <b>1.03</b>   | <b>1.52</b>   | <b>1.60</b>   | <b>1.52</b>   |
| Total tem area index                 | $\text{m}^2 \text{m}^{-2}$       | <b>0.51</b>   | <b>0.52</b>   | <b>0.51</b>   | <b>0.51</b>   | <b>0.51</b>   |
| Canopy height                        | m                                | <b>8.73</b>   | <b>8.73</b>   | <b>8.74</b>   | <b>8.73</b>   | <b>8.73</b>   |
| Surface stress                       | $\text{kg m}^{-1} \text{s}^{-2}$ | <b>0.007</b>  | <b>0.011</b>  | <b>0.007</b>  | <b>0.009</b>  | <b>0.008</b>  |
| Surface albedo                       | fraction                         | <b>−0.022</b> | <b>−0.030</b> | <b>−0.021</b> | <b>−0.019</b> | <b>−0.023</b> |
| Surface net downward shortwave flux  | $\text{W m}^{-2}$                | <b>3.52</b>   | <b>5.34</b>   | 0.98          | 2.16          | <b>5.48</b>   |
| Surface downward shortwave flux      | $\text{W m}^{-2}$                | −0.61         | 2.44          | <b>−4.12</b>  | <b>−3.11</b>  | <b>2.22</b>   |
| Surface upward shortwave flux        | $\text{W m}^{-2}$                | <b>−4.13</b>  | <b>−2.91</b>  | <b>−5.10</b>  | <b>−5.27</b>  | <b>−3.26</b>  |
| Surface net upward longwave flux     | $\text{W m}^{-2}$                | −0.63         | 1.79          | <b>−1.96</b>  | <b>−2.67</b>  | 0.20          |
| Heat flux into soil layers           | $\text{W m}^{-2}$                | −0.03         | 0.25          | <b>−0.96</b>  | <b>−0.33</b>  | <b>0.89</b>   |
| Total sensible heat flux             | $\text{W m}^{-2}$                | <b>2.34</b>   | <b>2.12</b>   | <b>2.54</b>   | <b>1.94</b>   | <b>2.77</b>   |
| Sensible heat flux from ground       | $\text{W m}^{-2}$                | <b>−2.18</b>  | <b>−2.28</b>  | <b>−2.32</b>  | <b>−2.07</b>  | <b>−2.04</b>  |
| Sensible heat flux from vegetation   | $\text{W m}^{-2}$                | <b>4.52</b>   | <b>4.39</b>   | <b>4.86</b>   | <b>4.00</b>   | <b>4.82</b>   |
| Total latent heat flux               | $\text{W m}^{-2}$                | <b>1.85</b>   | <b>1.18</b>   | <b>1.37</b>   | <b>3.22</b>   | <b>1.62</b>   |
| Latent heat from transpiration       | $\text{W m}^{-2}$                | <b>4.04</b>   | <b>1.27</b>   | <b>4.07</b>   | <b>7.17</b>   | <b>3.65</b>   |
| Latent heat from canopy evaporation  | $\text{W m}^{-2}$                | <b>2.22</b>   | <b>0.72</b>   | <b>2.58</b>   | <b>4.28</b>   | <b>1.31</b>   |
| Latent heat from ground evaporation  | $\text{W m}^{-2}$                | <b>−4.42</b>  | <b>−0.81</b>  | <b>−5.28</b>  | <b>−8.23</b>  | <b>−3.35</b>  |
| Surface air temperature              | $^{\circ}\text{C}$               | −0.11         | 0.10          | −0.16         | <b>−0.30</b>  | −0.11         |
| Precipitation                        | $\text{mm day}^{-1}$             | 0.02          | −0.21         | 0.16          | <b>0.23</b>   | −0.12         |
| Precipitable water                   | $\text{kg m}^{-2}$               | 0.18          | −0.28         | 0.30          | <b>0.70</b>   | 0.01          |
| Convective precipitation             | $\text{mm day}^{-1}$             | 0.04          | −0.06         | 0.03          | <b>0.21</b>   | −0.02         |
| Large-scale precipitation            | $\text{mm day}^{-1}$             | −0.02         | −0.15         | <b>0.13</b>   | 0.02          | −0.10         |
| Total evapotranspiration             | $\text{mm day}^{-1}$             | <b>0.06</b>   | <b>0.03</b>   | <b>0.05</b>   | <b>0.11</b>   | <b>0.05</b>   |
| Ground evaporation                   | $\text{mm day}^{-1}$             | <b>−0.15</b>  | <b>−0.03</b>  | <b>−0.18</b>  | <b>−0.28</b>  | <b>−0.12</b>  |
| Canopy evaporation                   | $\text{mm day}^{-1}$             | <b>0.08</b>   | <b>0.02</b>   | <b>0.09</b>   | <b>0.15</b>   | <b>0.05</b>   |
| Canopy transpiration                 | $\text{mm day}^{-1}$             | <b>0.14</b>   | <b>0.04</b>   | <b>0.14</b>   | <b>0.25</b>   | <b>0.12</b>   |
| Precipitation minus evaporation      | $\text{mm day}^{-1}$             | −0.04         | −0.24         | 0.12          | 0.12          | <b>−0.17</b>  |
| Total runoff                         | $\text{mm day}^{-1}$             | −0.05         | −0.14         | −0.02         | 0.01          | −0.02         |
| Total volumetric soil moisture       | $\text{mm}^3 \text{mm}^{-3}$     | <b>−0.007</b> | <b>−0.010</b> | <b>−0.007</b> | −0.005        | <b>−0.005</b> |
| Vertical velocity at 500 hPa         | $\text{Pa s}^{-1}$               | 0.000         | 0.003         | −0.003        | <b>−0.002</b> | 0.002         |
| Convective cloud fraction at 500 hPa | fraction                         | 0.001         | −0.001        | 0.000         | <b>0.003</b>  | 0.000         |
| Total cloud cover fraction           | fraction                         | −0.002        | −0.024        | <b>0.014</b>  | <b>0.017</b>  | <b>−0.012</b> |

This process provides more water vapor available for precipitation, though the water vapor is not a limited resource for precipitation in the SEUS.

During JJA, there are no significant changes in precipitation minus evaporation, total runoff, or total soil moisture. However, total soil moisture is significantly decreased in other seasons ( $−0.007 \text{ mm}^3 \text{mm}^{-3}$  in MAM,  $−0.005 \text{ mm}^3 \text{mm}^{-3}$  in SON, and  $−0.01 \text{ mm}^3 \text{mm}^{-3}$  in DJF, Table 2), which indicates the ability of trees to access deep moisture in the soil.

By comparing Fig. 3a and Fig. 3b, one can see that precipitation in JJA significantly decreases over regions adjacent to the SEUS, to the north and west in the long term (Fig. 3b). The west regions adjacent to the SEUS include Utah, New Mexico, and northwest of Texas. The north regions adjacent to the SEUS include Iowa, south of Wisconsin, north of Illinois, south of Michigan, north of Indiana, and Ohio. This is a remote effect of afforestation over the SEUS. The decreases in precipitation over the adjacent regions are caused by the significant

descending anomalies generated over the adjacent regions around the SEUS (Fig. 4a). These descending anomalies are generated to compensate the air lost near the surface over the SEUS because of the local ascending anomaly. With these descending anomalies, convective cloud cover, total cloud cover, and precipitation significantly decline over the adjacent regions. While precipitation change is not significant over the adjacent regions in Fig. 3a, it does show a decrease in precipitation. The reduction in precipitation explains the decrease in total tree cover (Fig. 2a) and the increase in total grass cover over the west adjacent regions (Fig. 2b). By the descending anomaly over the west adjacent region, the North American monsoon system could be dampened.

## 2) SURFACE TEMPERATURE CHANGE

Long-term surface air temperature significantly decreases by  $−0.30^{\circ}\text{C}$  in JJA over the SEUS (Table 2,

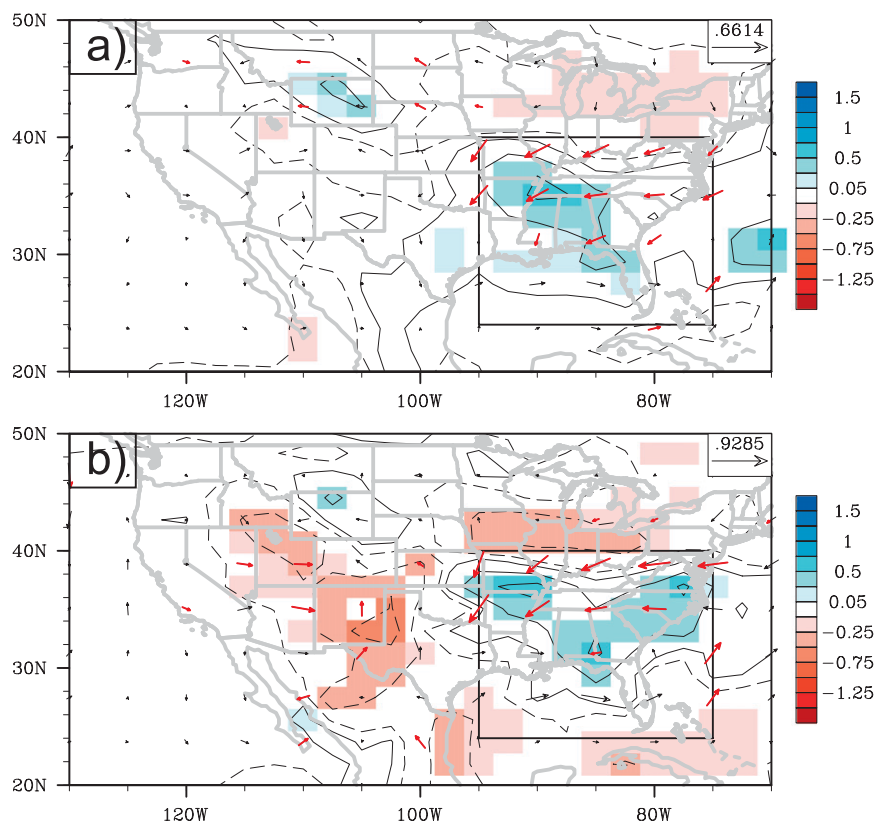


FIG. 3. (a) Short-term (HTC – ENS) and (b) long-term (HTC – LTC) differences in precipitation (color shading and contours:  $\text{mm day}^{-1}$ ) and surface wind (vectors:  $\text{m s}^{-1}$ ) in JJA. Color shading is only shown for statistically significant changes in precipitation ( $P < 0.1$ ). Red vectors indicate statistically significant changes in wind speed ( $P < 0.1$ ).

Fig. 5b). The decrease in surface air temperature is even greater in the short term (Fig. 5a). The cooling effect of afforestation over the SEUS can be explained by the aforementioned three mechanisms. The decrease in surface albedo ( $-0.019$ ) in JJA causes the surface upward shortwave flux to decrease by  $-5.27 \text{ W m}^{-2}$  (Table 2). However, the surface downward shortwave flux decreases by  $-3.11 \text{ W m}^{-2}$  owing to more clouds being produced ( $+0.017$ ) in the atmosphere (Table 2, Figs. 4b,c). Thus, the net surface downward shortwave flux only increases by  $+2.16 \text{ W m}^{-2}$  in JJA (not significant). So the lower albedo would warm the surface. But the increase in the turbulent fluxes (latent heat flux + sensible heat flux) is  $+5.16 \text{ W m}^{-2}$  ( $+1.94 \text{ W m}^{-2}$  in sensible heat flux and  $+3.22 \text{ W m}^{-2}$  in latent heat flux). Overall, the increase in the net surface downward shortwave flux is less than the increase in turbulent fluxes at the surface, so the surface air temperature is reduced. As a result, the net surface upward longwave flux decreases by  $-2.67 \text{ W m}^{-2}$  (Table 2). The increase in the turbulent fluxes is mainly attributed to the higher evapotranspiration with afforestation

(evapotranspiration mechanism). The increase in the sensible heat flux may be due to a higher mechanical mixing caused by the rougher surface (Delire et al. 2002) (roughness mechanism), which needs further study in fully coupled models. The sensible heat change and the latent heat change are in the same direction in our study, similar to the study by Hoffmann and Jackson (2000), in which savannas were converted into grassland over North Australia, North Africa, and South America in the NCAR CCM3 land surface model (LSM).

By comparing Fig. 5a and Fig. 5b, one also can identify the remote effect of afforestation on temperature (Fig. 5b). Temperature significantly increases over the adjacent regions around the SEUS, which is mainly caused by adiabatic warming from subsidence and the reduction in total cloud cover (Figs. 4b,c). Temperature also increases in Fig. 5a over the adjacent regions, though the change is not significant. This remote adjacent warming may cancel the local cooling over the SEUS in the long term, which explains that the cooling effect is stronger in the short term.

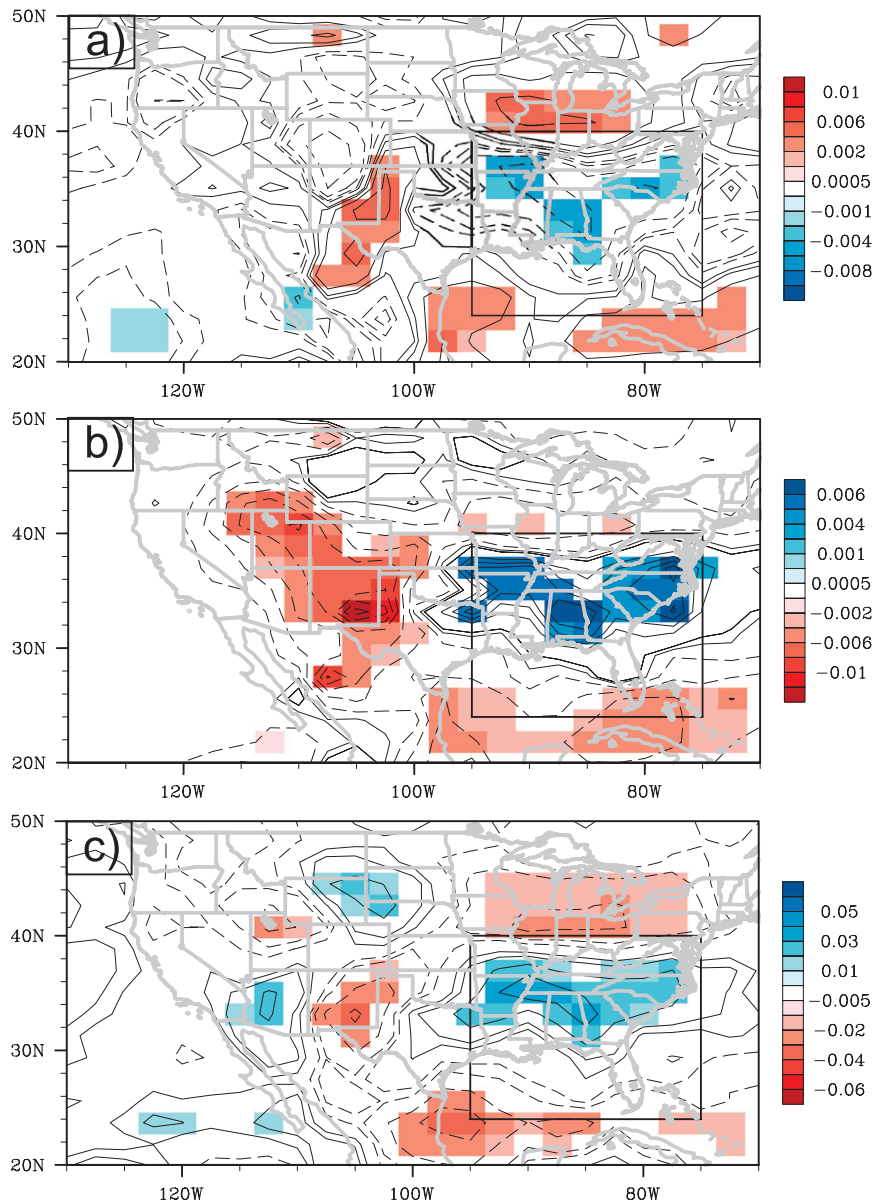


FIG. 4. Long-term (HTC - LTC) differences in (a) vertical velocity at 500 hPa (color shading and contours:  $\text{Pa s}^{-1}$ ), (b) convective cloud cover fraction at 500 hPa (color shading and contours), and (c) total cloud cover fraction (color shading and contours) in JJA. Color shading is only shown for statistically significant changes in (a) vertical velocity, (b) convective cloud cover fraction, and (c) total cloud cover fraction ( $P < 0.1$ ).

#### 4. Summary and discussion

The potential effects of afforestation over the SEUS are assessed by two long-term quasi-equilibrium experiments and 80 initial value ensemble experiments with a fully coupled GCM. In one of the two long-term quasi-equilibrium experiments, the total maximum tree cover for each grid is capped at 95% globally (model default). In the other long-term quasi-equilibrium

experiments and all the ensemble experiments, the total maximum tree cover for each grid is capped at 95% too, except that the total maximum tree cover for each grid is capped at 65% in the SEUS.

Our model results show that afforestation over the SEUS produces local effects at both short and long time scales and also produces remote effects at a long time scale in summer. The short-term and long-term local effects are that afforestation over the SEUS lowers



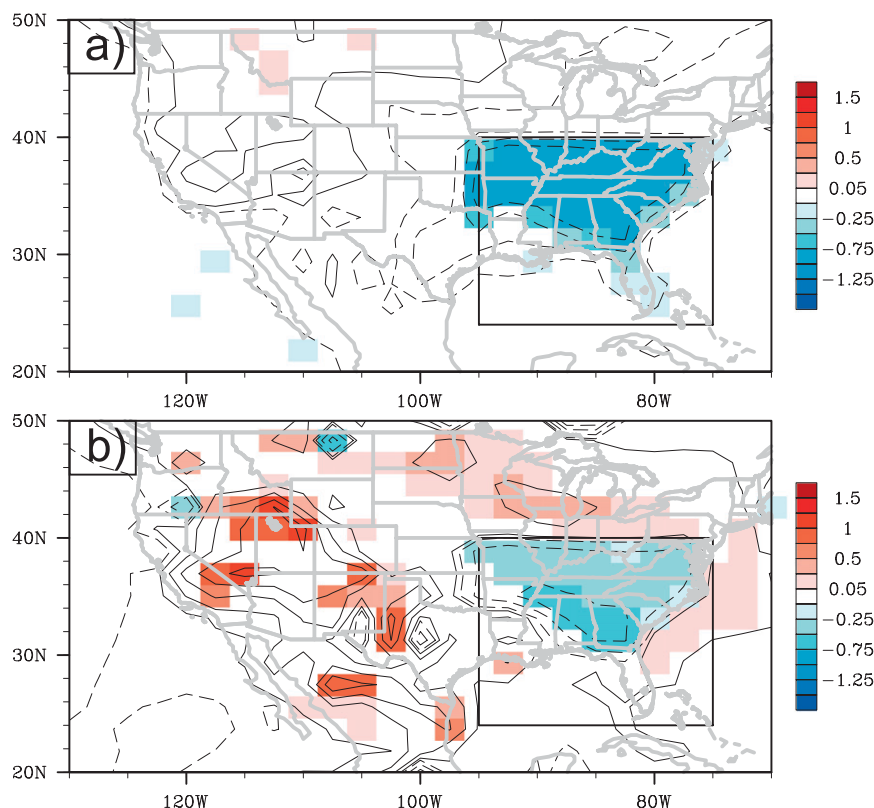


FIG. 5. (a) Short-term (HTC – ENS) and (b) long-term (HTC – LTC) differences in surface air temperature (color shading and contours: °C) in JJA. Color shading is only shown for statistically significant changes in surface air temperature ( $P < 0.1$ ).

surface air temperature and increases precipitation in summer. Though it is hard to distinguish whether the increase in precipitation is mainly due to the roughness mechanism or the evapotranspiration mechanism in the fully coupled model, it seems that the change in roughness length has the greatest influence on precipitation in moist areas, such as the SEUS, suggested by the studies of Betts (1998). Future experiments are needed to prove the roughness mechanism in the SEUS. The short-term remote effects on temperature and precipitation are not significant. But the long-term remote effects generate an increase in the surface air temperature and a decrease in precipitation over the adjacent regions of the Southeast United States (the Southwest United States and the Midwest United States) in summer. It is worth pointing out that the ocean effects are not clear in these experiments. However, our work on afforestation effects over the East Asian monsoon shows that ocean plays an important role on precipitation and temperature changes by altering SSTs (D. Ma et al. 2012, unpublished manuscript).

The potential effects of afforestation on temperature over the SEUS found here are consistent with the

observation data (Notaro and Liu 2006) and most simulated results (Xue et al. 1996; Copeland et al. 1996; Baidya Roy et al. 2003; Jackson et al. 2005; Liu 2011). The potential effects of afforestation on precipitation are also consistent with the observation data (Notaro and Liu 2006) and some of the model results (e.g., Xue et al. 1996). However, the local and remote changes in summertime precipitation are generally opposite to the results obtained from a regional modeling study of afforestation over the southern United States by Liu (2011). He found that overall precipitation decreased in the SEUS and increased in the central Midwest in summer. Surface air temperature decreased in the SEUS in summer, but only slightly. Nevertheless, he did find that precipitation increased in the eastern portion of the SEUS, which is consistent with our finding. The differences between the two simulations are possible because of the type of vegetation changed and the area of afforestation simulated. The type of vegetation changed in Liu (2011) was crops to trees and grasses to trees in our simulation. The area of afforestation simulated in Liu (2011) was mostly along the Gulf coast, which was much smaller than in our simulation. Another reason for the

difference in precipitation might be that moisture recycling in CCSM3.5 is stronger than that in Regional Climate Model (RegCM). Moisture recycling is observed to be strong over the SEUS, about two times as strong as the global land mean (Trenberth 1999). Therefore with similar changes in the surface wind (cyclonic circulation), CCSM3.5 produces more precipitation over the SEUS. Though the detail reasons for the differences need to be further explored, it suggests that it would be a better to study regional afforestation effects by combining GCMs and RegCMs.

The local effect on precipitation is also different from the study by Jackson et al. (2005). They found that precipitation decreases with afforestation over temperate regions because temperate regions lack sufficient energy to lift the additional atmospheric moisture high enough to condense and form clouds. In our study region, however, the climatology of vertical motion is ascent (figure not shown) and anomalous ascent is induced by the increase in roughness, so atmospheric moisture can be easily lifted high enough to condense and form clouds. Sud et al. (1988) found that precipitation decreases over the SEUS by reducing surface roughness, which is consistent with our finding. As further evidence, both total and convective cloud fractions increase over the SEUS (Fig. 4b).

The local changes in precipitation are not significant in other seasons (MAM, SON, and DJF). However, total soil moisture significantly decreases because of the ability of trees to access deep soil moisture. We note that there is a remote warming over the adjacent regions during winter (figure not shown), though there is no significant local wintertime effect (Table 2). This is probably caused by a decrease in evaporation efficiency, which is a function of soil water availability (Osborne et al. 2004). Our results show that precipitation decreases over the adjacent regions in summer. As a result, soil water availability in winter may be limited, which results in evaporation efficiency decrease, latent heat release decrease, and surface air temperature increasing.

The work presented here suggests that afforestation over the SEUS is a potential strategy to mitigate local greenhouse warming and reduce the intensity and frequency of severe heat waves (Meehl and Tebaldi 2004) by biophysical effects of vegetation. But the related remote effects of afforestation over adjacent regions could not be ignored. Remote hydrological cycle changes over the semiarid Southwest may have even greater societal impacts through changes in precipitation, evapotranspiration, runoff, and water availability for human use by suppressing the North American monsoon system. Therefore, planned afforestation efforts should be

developed carefully by taking account of short-term (local) and long-term (remote) biophysical effects of afforestation. This emphasizes the importance to coordinate forest management effort in the afforested region and the surrounding areas, as suggested by Liu et al. (2008). We note that the biochemical effect of afforestation over the SEUS on temperature is about  $0.04^{\circ}\text{C}$  and small relative to the biophysical effect. [Total carbon sequestered due to the afforestation over the SEUS is 21 Gigatonnes. Temperate changes  $0.002^{\circ}\text{C}$  Gigaton $^{-1}$  (Committee on Stabilization Targets for Atmospheric Greenhouse Gas Concentrations 2011).] However, the biophysical and the biochemical effect on temperature are in the same direction. Also it is worthy to point out that our experiment of LTC is a deforestation experiment from the potential vegetation over the SEUS. The potential vegetation outside of the SEUS may have effects on our finding. But we expect that this would not affect our main conclusions here. Future work is needed to test afforestation effects over the SEUS at different vegetation background scenarios.

**Acknowledgments.** The authors gratefully thank the three anonymous reviewers. Their comments and suggestions improved the paper significantly. This work is supported by USDA Forest Service and NOAA CPPA. This work is also supported by Grants GYHY200906016 and 2012CB955201. The simulations were made using NERSC computer resources. We thank Dr. Robert Gallimore for discussion.

## REFERENCES

- American Forest Congress, 1996: Southern region forest research report. *Proc. Seventh American Forest Congress*, Washington, D.C., AFC, 27 pp.
- Anderson, R., and Coauthors, 2010: Biophysical considerations in forestry for climate protection. *Front. Ecol. Environ.*, **9**, 174–182, doi:10.1890/090179.
- Avissar, R., and D. Werth, 2005: Global hydroclimatological teleconnections resulting from tropical deforestation. *J. Hydrometeor.*, **6**, 134–145.
- Baidya Roy, S., G. Hurtt, C. Weaver, and S. Pacala, 2003: Impact of historical land cover change on the July climate of the United States. *J. Geophys. Res.*, **108**, 4793, doi:10.1029/2003JD003565.
- Betts, R. A., 1998: Investigating the influence of vegetation on climate. Ph.D. thesis, University of Reading, 165 pp.
- , 2000: Offset of the potential carbon sink from boreal forestation by decreases in surface albedo. *Nature*, **408**, 187–190.
- Bonan, G. B., 1997: Effects of land use on the climate of the United States. *Climatic Change*, **37**, 449–486.
- , 2008: Forests and climate change: Forcings, feedbacks, and the climate benefits of forests. *Science*, **320**, 1444–1449.
- Canadell, J. G., and M. R. Raupach, 2008: Managing forests for climate change mitigation. *Science*, **320**, 1456–1457.

- Chapin, F., III, J. Randerson, A. McGuire, J. Foley, and C. Field, 2008: Changing feedbacks in the climate-biosphere system. *Front. Ecol. Environ.*, **6**, 313–320, doi:10.1890/080005.
- Charney, J. G., 1975: Dynamics of deserts and drought in the Sahel. *Quart. J. Roy. Meteor. Soc.*, **101**, 193–202.
- Chase, T. N., R. A. Pielke, T. G. F. Kittel, R. R. Nemani, and S. W. Running, 2000: Simulated impacts of historical land cover changes on global climate in northern winter. *Climate Dyn.*, **16**, 93–105.
- Committee on Stabilization Targets for Atmospheric Greenhouse Gas Concentrations, 2011: *Climate Stabilization Targets: Emission, Concentrations, and Impacts over Decades to Millennia*. National Academies Press, 298 pp.
- Copeland, J., R. Pielke, and T. G. F. Kittel, 1996: Potential climatic impacts of vegetation change: A regional modeling study. *J. Geophys. Res.*, **101**, 7409–7418.
- Costa, M. H. C., and J. A. Foley, 2000: Combined effects of deforestation and doubled atmospheric CO<sub>2</sub> concentrations on the climate of Amazonia. *J. Climate*, **13**, 18–34.
- Delire, C., S. Levis, G. Bonan, J. A. Foley, M. Coe, and S. Vavrus, 2002: Comparison of the climate simulated by the CCM3 coupled to two different land-surface models. *Climate Dyn.*, **19**, 657–669.
- Eltahir, E. A. B., and R. L. Bras, 1993: On the response of the tropical atmosphere to large-scale deforestation. *Quart. J. Roy. Meteor. Soc.*, **119**, 779–793.
- Field, C. B., D. B. Lobell, H. A. Peters, and N. R. Chiariello, 2007: Feedbacks of terrestrial ecosystems to climate change. *Annu. Rev. Environ. Resour.*, **32**, 1–29.
- Foley, J. A., M. H. Costa, C. Delire, N. Ramankutty, and P. Snyder, 2003: Green surprise? How terrestrial ecosystems could affect earth's climate. *Front. Ecol. Environ.*, **1**, 38–44.
- Gent, P. R., S. G. Yeager, R. B. Neale, S. Levis, and D. A. Bailey, 2010: Improvements in a half degree atmosphere/land version of the CCSM. *Climate Dyn.*, **34**, 819–833, doi:10.1007/s00382-009-0614-8.
- Gibbard, S., K. Caldeira, G. Bala, T. J. Phillips, and M. Wickett, 2005: Climate effects of global land cover change. *Geophys. Res. Lett.*, **32**, L23705, doi:10.1029/2005GL024550.
- Govindasamy, B., P. B. Duffy, and K. Caldeira, 2001: Land use changes and Northern Hemisphere cooling. *Geophys. Res. Lett.*, **28**, 291–294.
- Hack, J. J., 1994: Parameterization of moist convection in the National Center for Atmospheric Research community climate model (CCM2). *J. Geophys. Res.*, **99**, 5551–5568.
- , J. M. Caron, S. G. Yeager, K. W. Oleson, M. M. Holland, J. E. Truesdale, and P. J. Rasch, 2006: Simulation of the global hydrological cycle in the CCSM Community Atmosphere Model version 3 (CAM3): Mean features. *J. Climate*, **19**, 2199–2221.
- Hansen, M. C., R. S. Defries, J. R. G. Townshend, and R. Sohlberg, 2000: Global land cover classification at 1 km spatial resolution using a classification tree approach. *Int. J. Remote Sens.*, **21**, 1331–1364.
- Hasler, N., D. Werth, and R. Avissar, 2009: Effects of tropical deforestation on global hydroclimate: A multimodel ensemble analysis. *J. Climate*, **22**, 1124–1141.
- Hoffmann, W., and R. Jackson, 2000: Vegetation–climate feedbacks in the conversion of tropical savanna to grassland. *J. Climate*, **13**, 1593–1602.
- Jackson, R., and Coauthors, 2005: Trading water for carbon with biological carbon sequestration. *Science*, **310**, 1944–1947, doi:10.1126/science.1119282.
- Kaufmann, R. K., L. Zhou, R. B. Myneri, C. J. Tucker, D. Slayback, N. V. Shabanov, and J. Pinzon, 2003: The effect of vegetation on surface temperature: A statistical analysis of NDVI and climate data. *Geophys. Res. Lett.*, **30**, 2147, doi:10.1029/2003GL018251.
- Lawrence, D. M., P. E. Thornton, K. W. Oleson, and G. B. Bonan, 2007: The partitioning of evapotranspiration into transpiration, soil evaporation, and canopy evaporation in a GCM: Impacts on land–atmosphere interaction. *J. Hydrometeorol.*, **8**, 862–880.
- Lean, J., and P. R. Rowntree, 1993: A GCM simulation of the impact of Amazonian deforestation on climate using an improved canopy representation. *Quart. J. Roy. Meteor. Soc.*, **119**, 509–530.
- Levis, S., G. B. Bonan, and C. Bonfils, 2004: Soil feedback drives the mid-Holocene North African monsoon northward in fully coupled CCSM2 simulations with a dynamic vegetation model. *Climate Dyn.*, **23**, 791–802, doi:10.1007/s00382-004-0477-y.
- Lin, S.-J., 2004: A “vertically Lagrangian” finite-volume dynamical core for global models. *Mon. Wea. Rev.*, **132**, 2293–2307.
- Liu, Y.-Q., 2011: A numerical study on hydrological impacts of forest restoration in the Southern United States. *Ecohydrology*, **4**, 299–314, doi:10.1002/eco.178.
- , J. Stanturf, and H.-Q. Lu, 2008: Modeling the potential of the northern China forest shelterbelt in improving hydroclimate conditions. *J. Amer. Water Resour. Assoc.*, **44**, 1–17.
- Liu, Z., M. Notaro, J. Kutzbach, and N. Liu, 2006: Assessing global vegetation–climate feedback from observations. *J. Climate*, **19**, 787–814.
- Meehl, G., and C. Tebaldi, 2004: More intense, more frequent, and longer lasting heat waves in the 21st century. *Science*, **305**, 994–997.
- Notaro, M., and Z. Liu, 2006: Observed vegetation–climate feedbacks in the United States. *J. Climate*, **19**, 763–786.
- , and —, 2008: Statistical and dynamical assessment of vegetation feedbacks on climate over the boreal forests. *Climate Dyn.*, **31**, 691–712.
- , and D. Gutzler, 2011: Simulated impact of vegetation on climate across the North American monsoon region in CCSM3.5. *Climate Dyn.*, **38**, 795–814, doi:10.1007/s00382-010-0990-0.
- , G.-S. Chen, and Z. Liu, 2011a: Vegetation feedbacks to climate in the global monsoon regions. *J. Climate*, **24**, 5740–5756.
- , K.-H. Wyrwoll, and G.-S. Chen, 2011b: Did aboriginal vegetation burning impact on the Australian summer monsoon? *J. Geophys. Res.*, **38**, L11704, doi:10.1029/2011GL047774.
- Oleson, K. W., G. B. Bonan, S. Levis, and M. Vertenstein, 2004: Effect of land use change on North American climate: Impact of surface datasets and model biogeophysics. *Climate Dyn.*, **23**, 117–132, doi:10.1007/s00382-004-0426-9.
- , and Coauthors, 2008: Improvements to the community land model and their impact on the hydrological cycle. *J. Geophys. Res.*, **113**, G01021, doi:10.1029/2007JG000563.
- Osborne, T. M., D. M. Lawrence, J. M. Slingo, A. J. Challinor, and T. R. Wheeler, 2004: Influence of vegetation on the local climate and hydrology in the tropics: Sensitivity to soil parameters. *Climate Dyn.*, **23**, 45–61.
- Oyama, M. D., and C. A. Nobre, 2004: Climatic consequences of a large-scale desertification in northeast Brazil: A GCM simulation study. *J. Climate*, **17**, 3203–3213.

- Pacala, S., and R. Socolow, 2004: Stabilization wedges: Solving the climate problem for the next 50 years with current technologies. *Science*, **305**, 968–972.
- Ramankutty, N., and J. A. Foley, 1998: Characterizing patterns of global land use: An analysis of global cropland data. *Global Biogeochem. Cycles*, **12**, 667–685.
- Shukla, J., and Y. Mintz, 1982: Influence of land-surface evaporation on earth's climate. *Science*, **215**, 1498–1501.
- Snyder, P. K., 2010: The influence of tropical deforestation on the Northern Hemisphere climate by atmospheric teleconnections. *Earth Interact.*, **14**. [Available online at <http://EarthInteractions.org>.]
- Solomon, S., D. Qin, M. Manning, M. Marquis, K. Averyt, M. M. B. Tignor, H. L. Miller Jr., and Z. Chen, Eds., 2007: *Climate Change 2007: The Physical Science Basis*. Cambridge University Press, 996 pp.
- Stöckli, R., and Coauthors, 2008: Remote sensing data assimilation for a prognostic phenology model. *J. Geophys. Res.*, **113**, G04021, doi:10.1029/2008JG000781.
- Sud, Y. C., J. Shukla, and Y. Mintz, 1988: Influence of land surface roughness on atmospheric circulation and precipitation: A sensitivity study with a general circulation model. *J. Appl. Meteor.*, **27**, 1036–1054.
- Trenberth, K. E., 1999: Atmospheric moisture recycling: Role of advection and local evaporation. *J. Climate*, **12**, 1368–1381.
- Watson, T., 2009: Climate plan calls for forest expansion. *USA Today*, 19 August. [Available online at [http://www.usatoday.com/news/nation/environment/2009-08-19-forest\\_N.htm](http://www.usatoday.com/news/nation/environment/2009-08-19-forest_N.htm).]
- Werth, D., and R. Avissar, 2002: The local and global effects of Amazonian deforestation. *J. Geophys. Res.*, **107**, 8087, doi:10.1029/2001JD000717.
- Xue, Y., M. Fennessy, and P. J. Sellers, 1996: Impact of vegetation properties on U.S. summer weather prediction. *J. Geophys. Res.*, **101** (D3), 7419–7430.
- Zhang, G. J., and N. A. McFarlane, 1995: Sensitivity of climate simulations to the parameterization of cumulus convection in the Canadian Climate Centre general circulation model. *Atmos.–Ocean*, **33**, 407–446.